2-2022

Flexible Dye-Sensitized Solar Cells Assisted with Lead-Free Perovskite Halide

Judy Fan
Marshall University, x.fan@marshall.edu

Recommended Citation

Fan, X. Flexible dye-sensitized solar cells assisted with lead-free perovskite halide. Journal of Materials Research (2022). https://doi.org/10.1557/s43578-022-00501-9

Invited Paper

Flexible Dye-Sensitized Solar Cells Assisted with Lead-Free Perovskite Halide

Xiaojuan Fan*

Department of Physics, Marshall University, Huntington, WV 25755, USA

ABSTRACT

Dye-sensitized solar cells (DSSCs) have shown promising alternative to Si-based counterparts due to low cost, abundant raw materials, and non-vacuum processing. Here, we report a solution-based process to create flexible DSSCs on aluminum foils. Mesoporous TiO_2 electrode was directly deposited on Al foil through spin casting. After post-thermal annealing, the resultant samples render optical smooth, crack-free, and large nanocrystalline thin films. The as-prepared double-layer porous TiO_2 thin film was incorporated with a porphyrin dye followed by a perovskite halide salt Cs_2SnI_6, as the hole transport material, replacing liquid electrolyte. A transparent conducting plastic sheet was used as the cathodic electrode to complete the solar cell construction. Samples were characterized using X-ray diffraction, SEM, AFM, UV-Vis spectrometer, and current-voltage measurements. A photo-electricity conversion efficiency of 3.74% has been achieved that potentially makes the possibility of scaling up fabrication of all-solid-state flexible solar cells.

KEYWORDS: Flexible solar cells, dye-sensitizer, hole transport materials, solar energy conversion.

* Author to whom correspondence should be addressed. E-mail: fan2@marshall.edu

I. INTRODUCTION

Dye-sensitized solar cells (DSSCs) have received increasing attentions in the past decades due to the features of low cost, fast process, light weight, non-toxicity, and abundant raw materials compared with other expensive semiconductor-based solar cells. In most of the solar cell productions, the fabrication usually requires high-vacuum and complex physical or chemical procedures, which is not in favor of large-scale manufactures. In contrast, DSSCs, as a promising alternative, can be processed in ambient environment using solution form. The pioneering work of DSSCs was reported in 1991 by Grätzel group, in which a solar cell device was fabricated on a mesoporous TiO_2 thin film covered by a charge transfer dye monolayer of Ru-based complex [1]. The device harvested solar light and yielded photo-electricity conversion efficiency of 7.9%. Later, the efficiency was improved up to 10% under AM 1.5 irradiation certified at the National Renewable Energy Laboratory in 1997. The dye molecular sensitizers of Ru-complex were designed to be easily linked onto metal oxide nanoparticles, while several other sensitizers, i.e. metal-free organic dyes, porphyrin dyes, and natural dyes were also introduced that can deliver a comparable efficiency at a lower cost [2-4]. Recently, a novel 3D plasmonic designation applied to the transparent electrode yielded an increased energy conversion efficiency [5]. Zhang group proved that photovoltage can be greatly lifted through the incorporation of Mn^{2+} into CdSe quantum dots attached on TiO_2 thin films [6]. Unlike semiconductor Si that acts as both sensitizer and transporter in traditional solar cells, metal oxide in DSSC, such as TiO_2, serves as both the porous structure anchoring dye molecules and the electrode transferring photocurrent as well as the absorber of ultraviolet light. Thus, metal oxide electrodes and dye molecules take the same important roles in the construction of DSSCs. Liquid electrolyte, commonly used in DSSCs, acts as the mediator to transfer iodide/triiodide redox couples that aims to suppress the

charge recombination. Despite the advantages of low-cost and fast process in DSSCs, organic and liquid materials if staying inside the optoelectronic devices often cause technique problems, such as sealing, leakage, corrosion, degradation, and limited lifetime. Therefore, various materials have been developed to replace the solvent-based liquid electrolytes, such as polymeric materials, quasi-solid-state ionic liquids, and perovskite hole transport materials (HTMs), so that all-solid-state, robust, and stable DSSCs can be made on flexible substrates [7-12]. Organometal halide perovskites used as photo sensitizer in solar cells were reported in 2009 for the first time [13]. Since then, this class of lead-based perovskite materials have been extensively investigated on solar cell applications by both experimental works and theoretical simulations [14-19]. For instance, anti-solvent engineering of organolead perovskites can significantly improve the performance of perovskite solar cells [20]. One of the rigid perovskite solar cells treated by the anti-solvent of compound ether could exhibit the power conversion efficiency (PCE) up to 18.47%, a very competitive result in current solar cell market [21]. A PCE of 13% was also achieved in a Br-substitution of I site organolead perovskite solar cells on glass substrates, where the whole fabrication can be processed at temperatures below 140°C [22]. Although organolead perovskite has been demonstrated the most efficient sensitizer in perovskite solar cell applications, the toxicity of lead-involved optoelectronic devices is a big problem that immediately urges further explorations of finding non-toxic substitutions, i.e., lead-free perovskite alternatives, such as Sn^{2+} based perovskites including $CH_3NH_3SnI_3$, $CH_3NH_3BiI_3$, $FASnI_3$, and $CsSnI_3$ [23-30]. Unfortunately, Sn^{2+} based perovskite halides exhibit a poor stability and fast degradation due to the rapid oxidation of Sn^{2+} to Sn^{4+} in air. Instead, a lead-free double perovskite halide of Cs_2SnI_6 is found to be more stable than $CsSnI_3$ in air but with similar transportation and light absorption regime. It was reported that the first Cs_2SnI_6-based all-solid-

state solar cells were successfully created with a delicate PCE of near 1% [31]. After that, Cs_2SnI_6 has received enthusiastic investigations and the PCE was improved to 4.7% by using it as the hole transporter in rigid glass-based DSSCs . Further studies on Sn-based devices concluded that the cell performance can be greatly enhanced by reducing recombination centers in both layer matrix and interfaces. In addition, its excellent optoelectronic properties have facilitated other applications beyond photovoltaics, such as photodetectors and photocatalysts [32-36]. However, incorporating Cs_2SnI_6 as a hole transporter in flexible solar cells, especially flexible DSSCs on Al foils, has not been extensively studied.

So far, the best efficiency of 12% was obtained from DSSCs built on rigid glass substrates with liquid electrolytes [1, 37-40]. The first ever flexible DSSC using Z907 dye sensitizer and eutectic melt electrolyte showed a PCE of 6.5% [41]. Flexible solar cells if created on opaque substrates would need backside incident irradiation through cathodic electrodes [42-46]. Transparent plastic poly(ethylene terephthalate) (PET) sheet was one of such cathodic electrode materials for backside illumination amid opaque anodes [47]. Some conductive substrates can only be used as cathodic electrodes in flexible DSSCs due to low temperature sustaining and poor adhesion. To overcome these shortages, new methods have been developed and implemented, such as facile electrodeposition, screen printing, ink-jet printing, electrospray, and so on. For instance, DSSCs were created on plastic ITO-PEN sheets by spray-coating of Pt as the cathodic electrode, which could yield a PCE of 8.5% [48]. Moreover, a quasi-solid-state DSSC coupled with an optimized PET film displayed a high PCE of 10.25% [49]. Owing to good flexibility, transparency, and fast-processing, polymeric materials have proved themselves the optimal components used in flexible DSSCs, which can deliver reasonable PCEs under visible light irradiation [50-53]. However, all plastic polymer solar cells

may encounter composite degradations and strength reductions at high temperatures or under harsh weather conditions during outdoor operations. On the contrary, flexible metallic substrates often exhibit excellent flexibility, ductility, durability, and thermal stability, such as titanium, platinum, nickel, aluminum, copper, and stainless steel. Electrically anodized titanium foils used as anodes have been reported that through the back-illumination, the energy conversion efficiency has reached to 7.1% [54-56]. Although carrier transportation in bulk TiO_2 crystals remains low due to the large band gap (3.2 eV), porous nanocrystalline TiO_2 thin film, an adoptive structure for DSSCs, can vastly host dye molecules on the large surface areas of the pores, where the matching energy band structures between TiO_2 nanoparticles and dye molecules allow photocurrent easily transferring from dye molecules to TiO_2 nanoparticles with limited recombination. In a recent work, energy storage devices were proposed to have an enhanced transportation based on highly conductive and flexible TiO_2-Carbon nanotube sheets, however, no practical application was presented on solar cell fabrications in their work [57]. A flexible and transparent multilayer electrode TiO_2/Ag/ITO was successfully deposited on polyethylene terephthalate (PET) substates by RF magnetron sputtering system for photonic devices [58]. Single-crystalline anatase TiO_2 nanowire arrays grown on flexible titanium foils by hydrothermal method at 220°C and post thermal calcination at 600°C to 700°C were applied as the anodic electrodes in lithium ion batteries [59]. Therefore, direct deposition of porous TiO_2 nanocrystalline on metal Al foil substrates may be applied to the fabrications of flexible DSSCs. It is feasible to grow metal oxide thin films on flexible substrates by solution methods in ambient condition, which may offer a scalable process suitable to mass productions. Various metal foils and polymeric plastics substrates have been selected for the fabrication of flexible DSSCs through different procedures, but there is no report on direct deposition of porous TiO_2 thin films

on flexible metal foils in ambient environment followed by post thermal treatments. Among those metals, aluminum is the most abundant and affordable material that can sustain high annealing temperature of 500℃, a critical temperature to make TiO_2 anatase structure [60, 61]. The well-established method of using polymer or co-polymer as templates to deposit porous metal oxides on rigid glass substrates may now be transferred to flexible metal foils or plastic sheet substrates [62].This work reports a convenient, fast, and cost-effective method to build DSSCs on flexible Al foils through polymer-templated chemical solution processing, followed by a layer of Cs_2SnI_6 as the hole transport material to replace liquid electrolyte. All procedures were performed in ambient environment without the requirement of high-vacuum or glove box. The fabricated porous nanocrystalline TiO_2 thin films show uniform thickness, large area, and optical flat surface with crystalline TiO_2 particle size ranging from 30 nm to 200 nm. The flexible TiO_2 thin films stay in good adhesion with metallic Al foil substrates. The crystal structure of TiO_2 thin films was examined by X-Ray diffractometer (Rigaku, TX). Surface morphology images were carried out using Field Emission Scanning Electron Microscope (SEM) (JEOL, Japan) and Atomic Force Microscope (AFM) (NanoSurf, MA). Photo absorption spectrum was conducted using Cary 60 UV-Vis spectroscopy. Energy conversion efficiency were characterized through J-V curve measurements using Keithley 2400 source meter under one sun illumination (100 W/cm^2).

II. RESULTS AND DISCUSSIONS

A dense and thick nanocrystalline TiO_2 thin film on glass substrate was prepared using the same precursor for structure characterization purposes. The crystal structure was examined by X-Ray diffraction, as shown in Fig. 1, which reveals a good polycrystalline with major peaks at 2θ

values of 25.39°, 37.95°, 48.06°, 54.84°, and 62.83°, indicating TiO_2 nanoparticles in anatase phase. Anatase phase has been considered as the most effective structure for solar cell applications [63]. The crystallite size (d_{RX}) of the as-prepared thin film can be determined by the width measurement of the most intense peaks in the diffraction pattern according to Debye-Scherrer equation as follows:

$$d_{RX} = \frac{k\lambda}{\beta cos\theta}$$

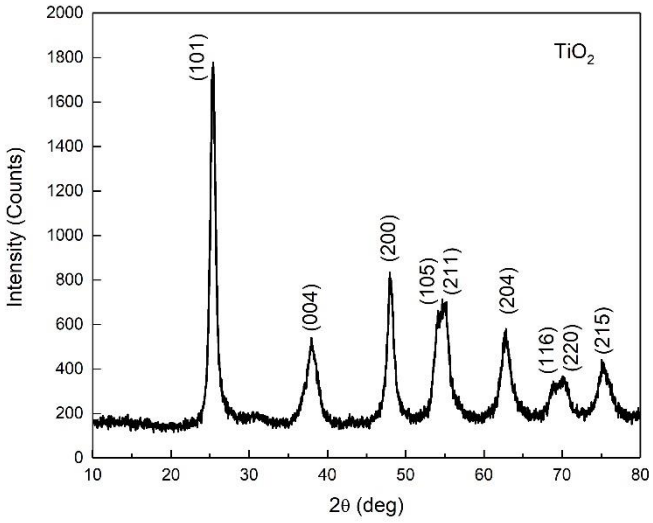

Figure 1: XRD pattern of TiO_2 nanocrystalline thin film on glass substrate.

where d_{RX} is the crystallite size, $k = 0.9$ is a correction factor which denotes the particle shape (spherical in this case), β is the full width at half maximum (FWHM, line broadening in radians) of the most intense diffraction peaks, λ is the wavelength of Cu target (0.15406 nm), and θ is the Bragg's angle. The quantitative results are summarized in table I. Crystal size ranges around 10 - 17 nm, which indicates that a high quality TiO_2 thin film with uniform crystallite size was realized.

Table 1: Average crystallite sizes of as prepared nanocrystalline TiO_2 thin film.

$2\theta°$	$\theta°$	$\beta(rad)$	d_{RX} (nm)
25.39	12.70	0.50	16.3
37.95	18.98	0.84	10.0
48.06	24.03	0.51	17.1
54.84	27.42	0.56	15.7
62.83	31.42	0.75	12.4

Cs_2SnI_6 is a double layer perovskite structure, slightly variant with the standard ABX_3 perovskite compounds [29]. The compound Cs_2SnI_6 is missing half of octahedral Sn atoms and therefore becomes a molecular salt with Sn^{4+} instead of Sn^{2+} contained in $CsSnI_3$ structure. This explicates the air-stability of the material. X-ray diffraction measurements on synthesized Cs_2SnI_6 black powder are displayed in Fig. 2, where the cubic $Fm\bar{3}m$ space group is adopted with a lattice constant around 11.67 Å. It has been reported that Cs_2SnI_6 is a p-type semiconductor possessing

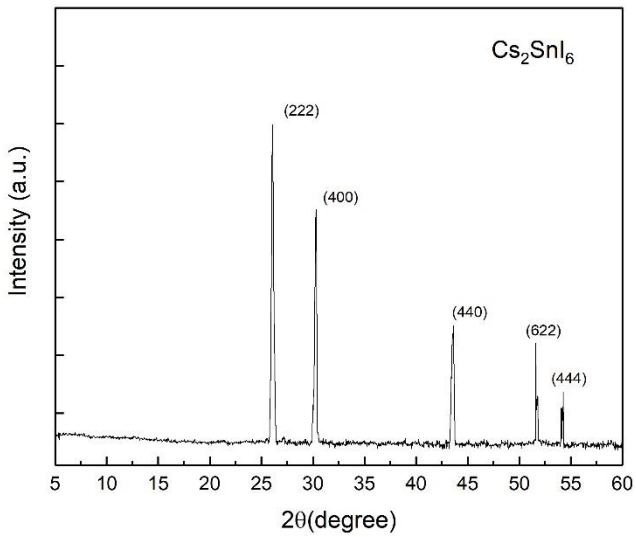

Figure 2. XRD pattern of Cs_2SnI_6 black powder.

a direct band gap with a value around 1.3 eV - 1.48 eV, in accordance with the broad peak position in its absorption spectrum .

Surface morphology of nanocrystalline TiO_2 thin films on glass substrates was examined by scanning electron microscope (SEM) and atomic force microscope (AFM) in both low and high magnifications. Fig.3a shows SEM micrographs in low magnification that the film has well distribution of TiO_2 nanoparticles in porous form with particles or particle clusters interconnected. Fig. 3b in high magnification depicts the particle size ranging from 200 nm to 500 nm with irregular pore shapes, i.e., a mesoporous structure built by spherical and interconnected nanocrystalline particles. The larger nanoparticle grain size and multiple layer appearances could be caused by multiple-step of spin-coating procedure and longer time of post-thermal treatment. EDS analysis confirms that the samples are mainly made of element Ti and oxygen, in agreement with the pure anatase TiO_2 crystal structure characterized by X-Ray diffraction. The sharp peak for element Sn is believed from the transparent conductive coating of FTO, while the prominent peaks labeled Ca and Si are the main compositions in glass substrate. No obvious large peaks come from other elements except those mentioned above, which demonstrates the as-grown samples being highly pure TiO_2 nanocrystals.

AFM images are displayed in Fig. 4a and 4b that were carried out on a different sample deposited on Al foil substrate from the same precursor and the same post-thermal temperature as the glass-based samples. Two images depict low (scan range 20μm×20μm) and high (scan range 2μm×2μm) magnifications, respectively. In addition, Fig. 4c illustrates the thin film surface roughness profile along the dash line shown in Fig. 4b, which reveals that the average nanoparticle size ranges from 20 nm – 100 nm, much less than the average size showed in SEM images probably due to thinner film by fewer repeating steps of spin-coating on this sample. The

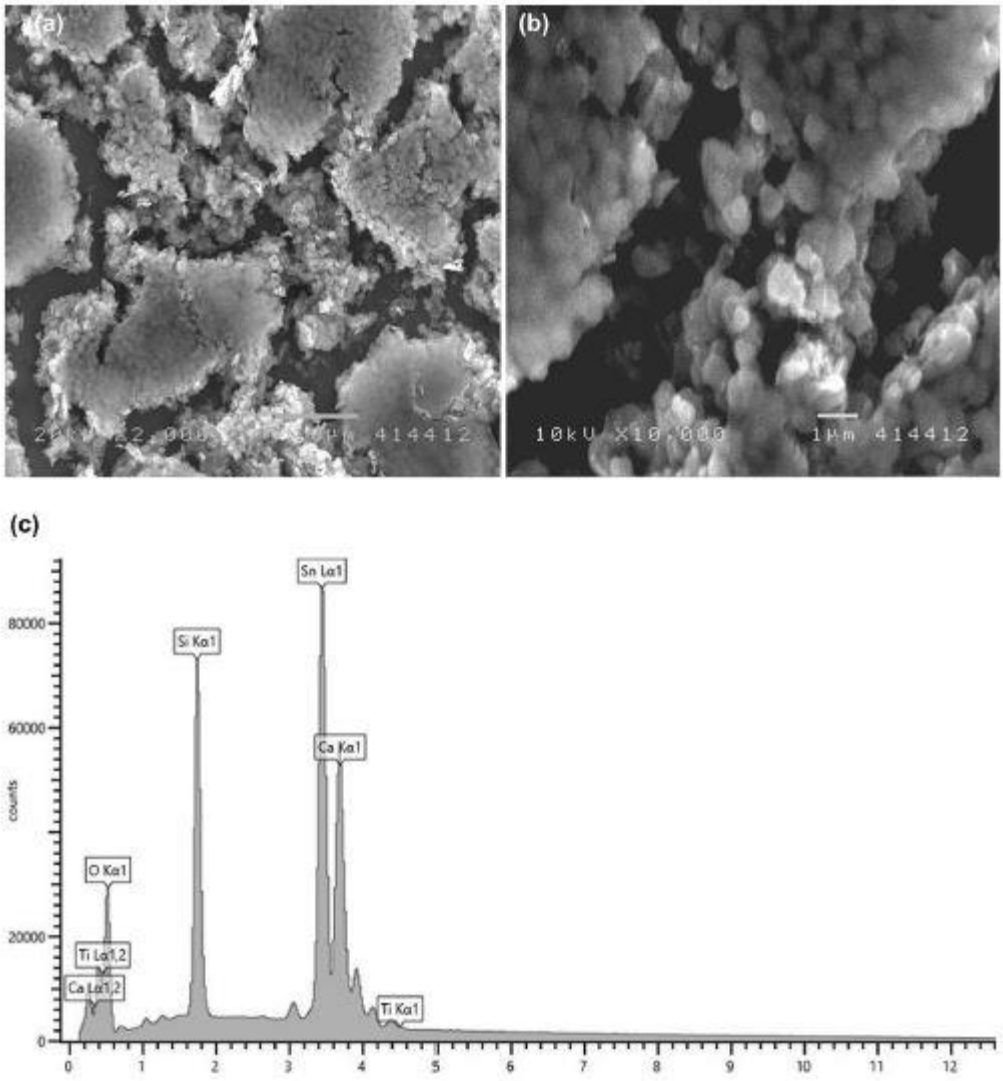

Figure 3. (a) Low magnification of SEM image, scale bar 10 μm; (b) High magnification of SEM image of porous TiO_2 thin films, scale bar 1 μm; (c) EDS analysis of confirmed elements in sample.

AFM images also indicate that the void area, i.e., pore size is at micrometer range in consistent with the SEM result presented in Fig. 3a. Large pore size provides spacious accommodation that favors more dye molecules easily anchoring on the spherical surfaces of TiO_2 nanoparticles.

The porphyrin dye N790 is a deep red (or purple) colored organic compound. Porphyrin derivatives are suitable for DSSC applications due to their unique thermal stability, excellent electronic transportation, and great absorption in visible light region [64]. The absorption

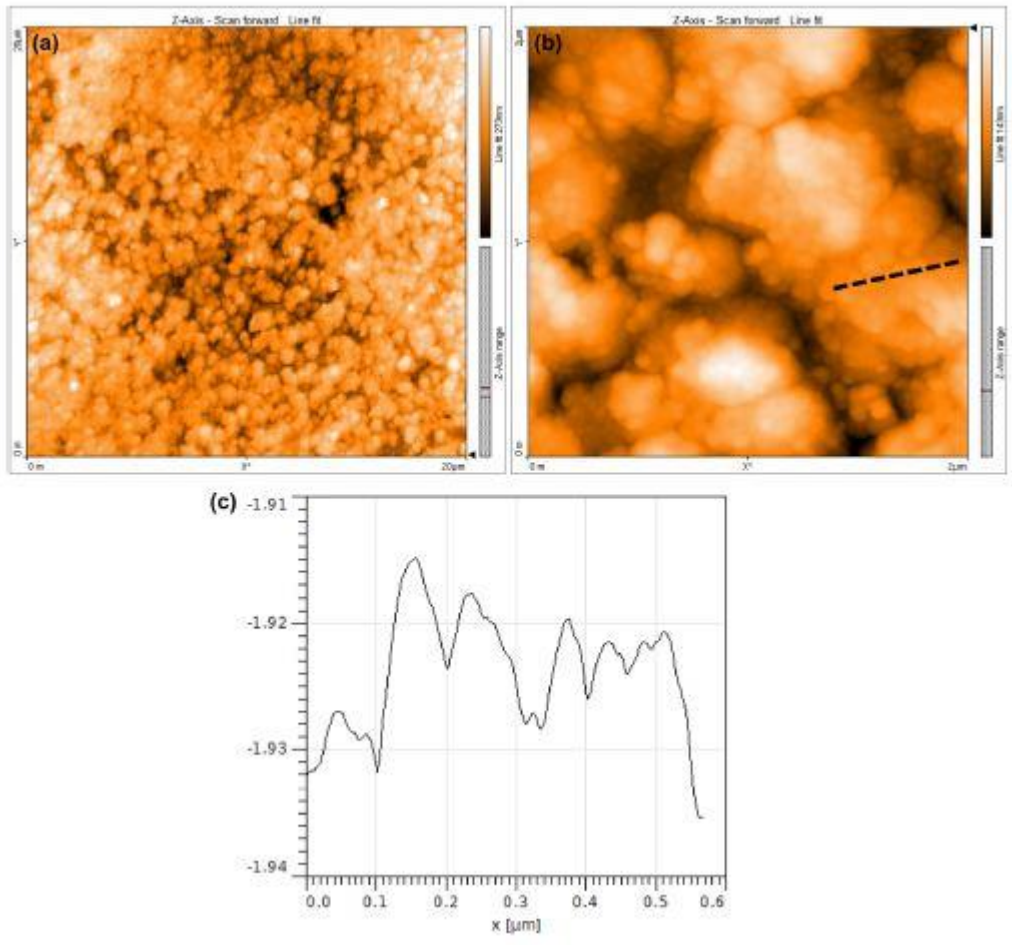

Figure 4. AFM image of TiO_2 nanoparticle thin film on Al foil substrate. (a) The image size is 20µm×20µm; (b) The image size is 2µm×2µm with a dash line as the guide for viewing the average nanoparticle size; (c) The profile of nanoparticles along the dash line shown in Fig. 4b.

spectrum was collected by UV-Vis spectrometer as shown in Fig. 5, in which a broad absorption spectrum is observed between 350 nm and 700 nm and peaked at 410 nm in accordance with its appearance of red-wine-color solution of molecular powder dissolved in ethanol. The same featured spectrum for N790 was also found in dye stained porous TiO_2 nanocrystalline solid-state thin films on Al foil substrates, which proves a good linkage status between the dye molecules and TiO_2 nanoparticles.

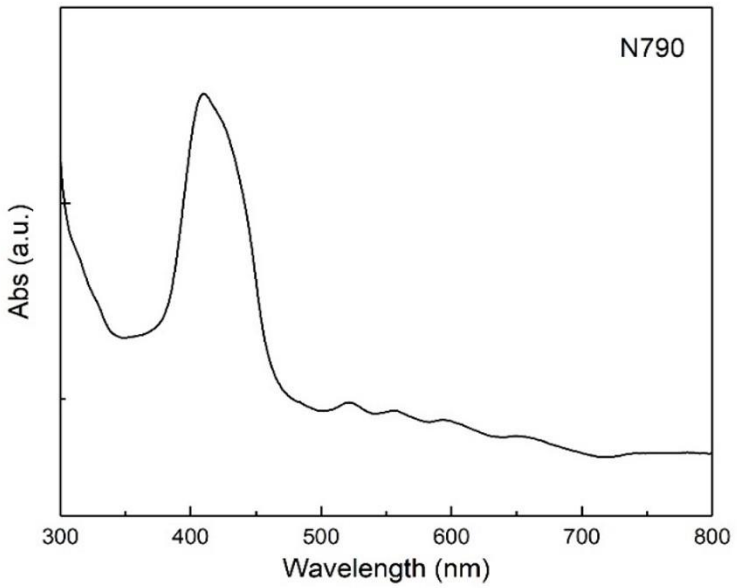

Figure 5. UV-Vis absorption spectroscopy of porphyrin dye N790.

Photo-energy conversion efficiency of the fabricated flexible DSSCs was characterized using Keithley 2400 source meter under a standard Sun light simulator. Due to the opaque feature of the Al foils, such solar cells need back side irradiation through the transparent PET sheet of cathode electrode. Fig. 6 displays a typical current-voltage measurement from one of the as-prepared solar cells under one sun light illumination, AM1.5, with the intensity at 100 mW/cm^2. The obtained result shows the short circuit current I_{sc} of ~ 6.72 mA/cm^2 and open circuit voltage V_{oc} ~ 0.83 V. The resultant fill factor is about 67% and the overall photo-energy conversion efficiency η is around 3.74%. The moderate efficiency may be explained in following aspects. In comparison with the higher efficiency of 6.5% in the Ru-dye based flexible DSSCs [41], the porphyrin N790 dye molecules used in this work is more affordable but less efficient. The reference of [42] also used costive titanium metal foils as the anode substrates and precious metal platinum underlayers, which are quite different with the cheaper and more abandoned aluminum foils. Through polymer templates and organometal precursors, the direct

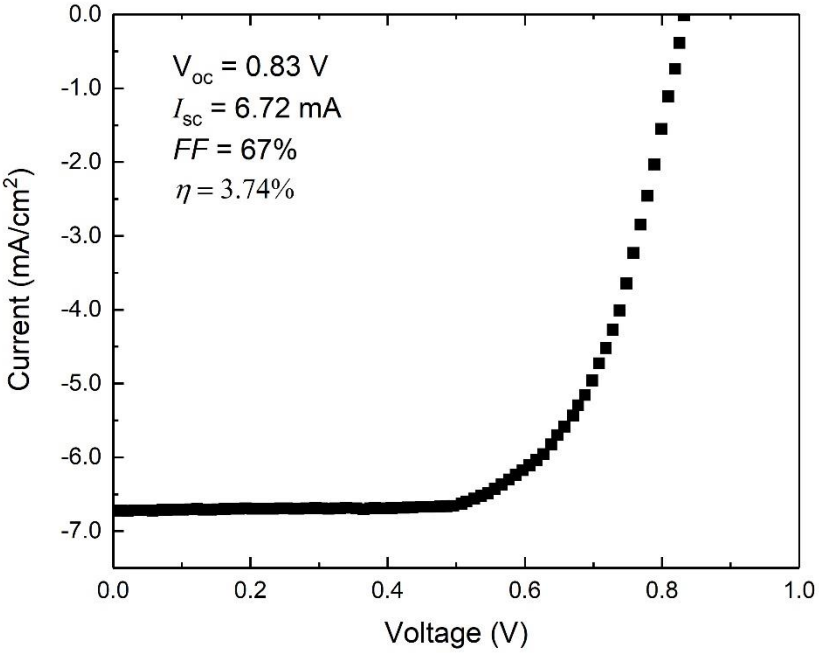

Figure 6. Current-voltage curve of the device under light intensity of one sun (AM1.5 global, 100 mW/cm^2).

depositions of large size and planar structure of TiO_2 thin films on Al foils may generate pin holes and impurities at both matrix layer and interfaces, which would inevitably increase device resistance and reduce carrier transportation. Extremely high-quality metal oxide thin films may require advanced equipment and high vacuum systems such as magnetron sputtering, e-beam evaporation, thermal evaporation, chemical vapor deposition, and etc. In a very similar work but different substrates, flexible DSSCs based on ZnO/TiO_2 core-shell structure deposited on stainless steel mesh yielded an optimal PCE of 2.84% [65]. They claimed that after an aluminum foil membrane was introduced on the back of the cell as a reflective layer, the efficiency was increased to 3.12%, revealing that the present work outperformed it upon the usage of aluminum foil substrates and easier processing. Another reason for the mild efficiency could be because the simple spreading method in ambient environment was adopted when the hole transport material Cs_2SnI_6 was laid on dye-stained TiO_2 thin films, which might create defects or non-contact areas

and likely affect the solar cell performance. Although high efficiencies mostly reported were realized in $CsSnI_3$-based solar cells, the instability of this material prevents the processing from ambient environment. Another example of Cs_2SnI_6 used as the hole transporter in glass-based DSSCs was able to deliver and maintain the PCE at 3.44% for several months without any sign of deformation, a proof of stability in air at room temperature [33]. This work incorporated the hole transport material of lead-free double-perovskite halide to Al foil-based flexible DSSCs through solution processing and achieved a better PCE than 3.44%, that may have demonstrated the possibility of scaling up production by this method. In conclusion, we have successfully fabricated flexible DSSCs on Al foils using mesoporous TiO_2 nanocrystalline thin films as the anodic electrodes made from polymer-templated chemical precursor. The thin film thickness can be controlled by both multiple spin-coating steps and the time duration of post thermal treatment. Pore size ranges from hundreds nanometer to a micron allowing more porphyrin dye molecules freely attached on the surfaces of TiO_2 nanoparticles to improve photovoltaic performance. Solid-state double-perovskite halide Cs_2SnI_6 serves as the hole transporter in the replacement of the liquid electrolyte to get rid of possible corrosion and leakage. With the backside irradiation, an energy conversion efficiency η = 3.74% has been achieved. The whole construction being operated in ambient environment is meaningful that has manifested a feasible step toward the realization of lead-free perovskite assisted flexible DSSCs on Al foils.

III. MATERIALS AND METHODS

General procedures of coating nanocrystalline TiO_2 on flexible Al foils start with a polymer template. Al foils were cleaned in isopropanol, and DI water in ultrasonication. Three weight percent polyethylene oxide (Sigma Aldrich) was dissolved in 20 ml of Toluene (Acros

Organics) by stirring, then mixed with six weight percent titanium butoxide (Sigma Aldrich). The mixture was vigorously stirred in a covered beaker for 2 hours. The resultant transparent and viscose solution was spun on cleaned Al foil substrates with backside taped on a Si wafer for surface flatting purpose. The casted thin films were heated up to 500°C in an oven for at least 4 hours. It is believed that all residual polymers and organics were removed thoroughly from the thin films after the high temperature annealing. Voids, i.e., pores, are left behind to render a porous structure with interconnected titania nanoparticles.

The lead-free and air-stable molecular iodosalt compound, Cs_2SnI_6, where Sn is in the 4^+ oxidation, provides a good replacement to the class of unstable perovskite halides. Cs_2SnI_6 compounds have a high-symmetry cubic structure with good air and moisture stability [12, 66]. Cs_2SnI_6 nanoparticle powder was synthesized through chemical solution route. The synthesis starts to mix 3.0 g Cs_2CO_3 in 20 mL aqueous HI to form a concentrated acidic solution of CsI. In another clean beaker, 3.1 g SnI_4 was dissolved in 10 mL absolute EtOH to obtain a clear orange solution. The mixture of the above two solutions was stirred vigorously until a precipitation of fine black particles appeared. Let the mixture stay in stirring for a further 120 min to ensure a thorough reaction completed. The final black powder was filtered off and washed with absolute EtOH by repeating three times. The obtained compound Cs_2SnI_6 after drying is moisture-stable at ambient environment.

As-prepared mesoporous TiO_2 thin films show smooth surface without any visible defects on which flexible DSSCs can be built. The photo sensitizer, meso-tetra(4-carboxyphenyl)-porphyrin dye (N790, 1mM solution in absolute ethanol), was attached on TiO_2 nanoparticles by merging the titania thin films into the dye solution for 24 hours until the surface turned to a deep-red color. A gel solution of Cs_2SnI_6 nanoparticles in PEG is drop-spread on the dye stained TiO_2

electrode surface and let it dry at 60ºC on a hot plate for 1 hour. A work area about 1×1 cm^2 was defined using resin glue and immediately sealed by a transparent conductive PET plastic sheet acting as the cathodic electrode to complete the solar cell fabrication.

Acknowledgements: This research was supported by NASA WV EPSCoR Program (sub-Grant # 216168) and NSF MU-ADVANCE (Grant # 0548113). The author also thanks Mr. David Neff, the technician, and Prof. Michael Norton for their generous help with the SEM images and EDS analyses in the Department of Chemistry at Marshall University.

Conflicts of Interest

This manuscript has not been published and is not under consideration for publication elsewhere. The author declares that there are no conflicts of interest regarding the publication of this article.

References:

[1] B. Oregan, M. Gratzel, A Low-Cost, High-Efficiency Solar-Cell Based on Dye-Sensitized Colloidal TiO2 Films, Nature, 353 (1991) 737-740.
[2] C.-L. Wang, Y.-C. Chang, C.-M. Lan, C.-F. Lo, E. Wei-Guang Diau, C.-Y. Lin, Enhanced light harvesting with π-conjugated cyclic aromatic hydrocarbons for porphyrin-sensitized solar cells, Energy & Environmental Science, 4 (2011) 1788-1795.
[3] S. Ito, S.M. Zakeeruddin, R. Humphry-Baker, P. Liska, R. Charvet, P. Comte, M.K. Nazeeruddin, P. Pechy, M. Takata, H. Miura, S. Uchida, M. Gratzel, High-efficiency organic-dye-sensitized solar cells controlled by nanocrystalline-TiO2 electrode thickness, Adv. Mater., 18 (2006) 1202-+.
[4] H. Chang, Y.-J. Lo, Pomegranate leaves and mulberry fruit as natural sensitizers for dye-sensitized solar cells, Solar Energy - SOLAR ENERG, 84 (2010) 1833-1837.
[5] Y.H. Sim, M.J. Yun, S.I. Cha, S.H. Seo, D.Y. Lee, Improvement in Energy Conversion Efficiency by Modification of Photon Distribution within the Photoanode of Dye-Sensitized Solar Cells, ACS Omega, 3 (2018) 698-705.
[6] C. Zhang, S. Liu, X. Liu, F. Deng, Y. Xiong, F.-C. Tsai, Incorporation of Mn(2+) into CdSe quantum dots by chemical bath co-deposition method for photovoltaic enhancement of quantum dot-sensitized solar cells, R Soc Open Sci, 5 (2018) 171712-171712.
[7] G.R.A. Kumara, A. Konno, K. Shiratsuchi, J. Tsukahara, K. Tennakone, Dye-Sensitized Solid-State Solar Cells: Use of Crystal Growth Inhibitors for Deposition of the Hole Collector, Chem. Mater., 14 (2002) 954-955.
[8] U. Bach, D. Lupo, P. Comte, J.E. Moser, F. Weissortel, J. Salbeck, H. Spreitzer, M. Gratzel, Solid-state dye-sensitized mesoporous TiO2 solar cells with high photon-to-electron conversion efficiencies, Nature, 395 (1998) 583-585.
[9] J.H. Wu, S. Hao, Z. Lan, J.M. Lin, M.L. Huang, Y.F. Huang, L.Q. Fang, S. Yin, T. Sato, A thermoplastic gel electrolyte for stable quasi-solid-state dye-sensitized solar cells, Advanced Functional Materials, 17 (2007) 2645-2652.
[10] K.F. Chen, C.H. Liu, H.K. Huang, C.H. Tsai, F.-R. Chen, Polyvinyl Butyral-Based Thin Film Polymeric Electrolyte for Dye-Sensitized Solar Cell with Long-Term Stability, International Journal of Electrochemical Science, 8 (2013) 3524-3539.
[11] N. Chander, P.S. Chandrasekhar, V.K. Komarala, Solid state plasmonic dye sensitized solar cells based on solution processed perovskite CsSnI3 as the hole transporter, RSC Advances, 4 (2014) 55658-55665.
[12] B. Lee, C.C. Stoumpos, N. Zhou, F. Hao, C. Malliakas, C.-Y. Yeh, T.J. Marks, M.G. Kanatzidis, R.P.H. Chang, Air-Stable Molecular Semiconducting Iodosalts for Solar Cell Applications: Cs2SnI6 as a Hole Conductor, J. Am. Chem. Soc., 136 (2014) 15379-15385.
[13] A. Kojima, K. Teshima, Y. Shirai, T. Miyasaka, Organometal Halide Perovskites as Visible-Light Sensitizers for Photovoltaic Cells, J. Am. Chem. Soc., 131 (2009) 6050-6051.
[14] J.H. Im, C.R. Lee, J.W. Lee, S.W. Park, N.G. Park, 6.5% efficient perovskite quantum-dot-sensitized solar cell, Nanoscale, 3 (2011) 4088-4093.
[15] M. Lee Michael, J. Teuscher, T. Miyasaka, N. Murakami Takurou, J. Snaith Henry, Efficient Hybrid Solar Cells Based on Meso-Superstructured Organometal Halide Perovskites, Science, 338 (2012) 643-647.
[16] B. Xia, Z. Wu, H. Dong, J. Xi, W. Wu, T. Lei, K. Xi, F. Yuan, B. Jiao, L. Xiao, Q. Gong, X. Hou, Formation of ultrasmooth perovskite films toward highly efficient inverted planar heterojunction solar cells by micro-flowing anti-solvent deposition in air, Journal of Materials Chemistry A, 4 (2016) 6295-6303.
[17] D. Schreurs, S. Nagels, I. Cardinaletti, T. Vangerven, R. Cornelissen, J. Vodnik, J. Hruby, W. Deferme, J.V. Manca, Methodology of the first combined in-flight and ex situ stability assessment of organic-based solar cells for space applications, Journal of Materials Research, 33 (2018) 1841-1852.

[18] I. Almansouri, M.A. Green, A. Ho-Baillie, The ultimate efficiency of organolead halide perovskite solar cells limited by Auger processes, Journal of Materials Research, 31 (2016) 2197-2203.
[19] S. Ahmed, J. Harris, J. Shaffer, M. Devgun, S. Chowdhury, A. Abdullah, S. Banerjee, Simulation studies of Sn-based perovskites with Cu back-contact for non-toxic and non-corrosive devices, Journal of Materials Research, 34 (2019) 2789-2795.
[20] M. Xiao, F. Huang, W. Huang, Y. Dkhissi, Y. Zhu, J. Etheridge, A. Gray-Weale, U. Bach, Y.B. Cheng, L. Spiccia, A fast deposition-crystallization procedure for highly efficient lead iodide perovskite thin-film solar cells, Angew Chem Int Ed Engl, 53 (2014) 9898-9903.
[21] J. Li, R. Yang, L. Que, Y. Wang, F. Wang, J. Wu, S. Li, Optimization of anti-solvent engineering toward high performance perovskite solar cells, Journal of Materials Research, 34 (2019) 2416-2424.
[22] T. Gotanda, S. Mori, H. Oooka, H. Jung, H. Nakao, K. Todori, Y. Nakai, Effects of gas blowing condition on formation of mixed halide perovskite layer on organic scaffolds, Journal of Materials Research, 32 (2017) 2700-2706.
[23] F. Hao, C.C. Stoumpos, D.H. Cao, R.P.H. Chang, M.G. Kanatzidis, Lead-free solid-state organic–inorganic halide perovskite solar cells, Nature Photonics, 8 (2014) 489-494.
[24] N.K. Noel, S.D. Stranks, A. Abate, C. Wehrenfennig, S. Guarnera, A.-A. Haghighirad, A. Sadhanala, G.E. Eperon, S.K. Pathak, M.B. Johnston, A. Petrozza, L.M. Herz, H.J. Snaith, Lead-free organic–inorganic tin halide perovskites for photovoltaic applications, Energy & Environmental Science, 7 (2014) 3061-3068.
[25] C.K. Kwak, A.T. Barrows, A.J. Pearson, D.G. Lidzey, A.D.F. Dunbar, An X-ray scattering and electron microscopy study of methylammonium bismuth perovskites for solar cell applications, Journal of Materials Research, 32 (2017) 1888-1898.
[26] S. Shao, J. Liu, G. Portale, H.-H. Fang, G.R. Blake, G.H. ten Brink, L.J.A. Koster, M.A. Loi, Highly Reproducible Sn-Based Hybrid Perovskite Solar Cells with 9% Efficiency, Advanced Energy Materials, 8 (2018) 1702019.
[27] L. He, H. Gu, X. Liu, P. Li, Y. Dang, C. Liang, L.K. Ono, Y. Qi, X. Tao, Efficient Anti-solvent-free Spin-Coated and Printed Sn-Perovskite Solar Cells with Crystal-Based Precursor Solutions, Matter, 2 (2020) 167-180.
[28] I. Chung, B. Lee, J. He, R.P.H. Chang, M.G. Kanatzidis, All-solid-state dye-sensitized solar cells with high efficiency, Nature, 485 (2012) 486-489.
[29] I. Chung, J.-H. Song, J. Im, J. Androulakis, C.D. Malliakas, H. Li, A.J. Freeman, J.T. Kenney, M.G. Kanatzidis, CsSnI3: Semiconductor or Metal? High Electrical Conductivity and Strong Near-Infrared Photoluminescence from a Single Material. High Hole Mobility and Phase-Transitions, J. Am. Chem. Soc., 134 (2012) 8579-8587.
[30] J. Zhang, C. Yu, L. Wang, Y. Li, Y. Ren, K. Shum, Energy barrier at the N719-dye/CsSnI3 interface for photogenerated holes in dye-sensitized solar cells, Scientific Reports, 4 (2014) 6954.
[31] X. Qiu, B. Cao, S. Yuan, X. Chen, Z. Qiu, Y. Jiang, Q. Ye, H. Wang, H. Zeng, J. Liu, M.G. Kanatzidis, From unstable CsSnI3 to air-stable Cs2SnI6: A lead-free perovskite solar cell light absorber with bandgap of 1.48eV and high absorption coefficient, Solar Energy Materials and Solar Cells, 159 (2017) 227-234.
[32] S.T. Umedov, A.V. Grigorieva, L.S. Lepnev, A.V. Knotko, K. Nakabayashi, S.-i. Ohkoshi, A.V. Shevelkov, Indium Doping of Lead-Free Perovskite Cs2SnI6, Frontiers in Chemistry, 8 (2020) 564.
[33] A. Kaltzoglou, D. Perganti, M. Antoniadou, A.G. Kontos, P. Falaras, Stress Tests on Dye-sensitized Solar Cells with the Cs2SnI6 Defect Perovskite as Hole-transporting Material, Energy Procedia, 102 (2016) 49-55.
[34] X.D. Wang, W.G. Li, J.F. Liao, D.B. Kuang, Recent Advances in Halide Perovskite Single-Crystal Thin Films: Fabrication Methods and Optoelectronic Applications, Solar RRL, 3 (2019) 1800294.
[35] T.C. Dang, H.C. Le, D.L. Pham, S.H. Nguyen, T.T.O. Nguyen, T.T. Nguyen, T.D. Nguyen, Synthesis of perovskite Cs2SnI6 film via the solution processed approach: First study on the photoelectrochemical water splitting application, Journal of Alloys and Compounds, 805 (2019) 847-851.

[36] X. Han, J. Liang, J.-H. Yang, K. Soni, Q. Fang, W. Wang, J. Zhang, S. Jia, A.A. Martí, Y. Zhao, J. Lou, Lead-Free Double Perovskite Cs2SnX6: Facile Solution Synthesis and Excellent Stability, Small, 15 (2019) 1901650.
[37] C. Lv, X. Wang, Q. Li, C. Li, Q. Ouyang, Y. Liu, L. Qi, Template-assisted synthesis of porous TiO2 photoanode for efficient dye-sensitized solar cells, Journal of Materials Research, 35 (2020) 2138-2147.
[38] X. Wu, G. Lu, L. Wang, The effect of photoanode thickness on the performance of dye-sensitized solar cells containing TiO2 nanosheets with exposed reactive {001} facets, Journal of Materials Research, 28 (2013) 475-479.
[39] J. Manju, S.M.J. Jawhar, Synthesis of magnesium-doped TiO2 photoelectrodes for dye-sensitized solar cell applications by solvothermal microwave irradiation method, Journal of Materials Research, 33 (2018) 1534-1542.
[40] M.J. Yun, Y.H. Sim, S.I. Cha, S.H. Seo, D.Y. Lee, High Energy Conversion Efficiency with 3-D Micro-Patterned Photoanode for Enhancement Diffusivity and Modification of Photon Distribution in Dye-Sensitized Solar Cells, Scientific Reports, 7 (2017) 15027.
[41] M. Wang, A.M. Anghel, B. Marsan, N.L. Cevey Ha, N. Pootrakulchote, S.M. Zakeeruddin, M. Grätzel, CoS supersedes Pt as efficient electrocatalyst for triiodide reduction in dye-sensitized solar cells, J Am Chem Soc, 131 (2009) 15976-15977.
[42] Y.H. Lin, Y.C. Wu, H.C. You, P.H. Chen, Y.H. Tsai, B.Y. Lai, Ultra-low Temperature Flexible Dye-Sensitized Solar Cell, 2014 International Symposium on Computer, Consumer and Control, 2014, pp. 470-473.
[43] M.J. Yun, S.I. Cha, S.H. Seo, D.Y. Lee, Highly Flexible Dye-sensitized Solar Cells Produced by Sewing Textile Electrodes on Cloth, Scientific Reports, 4 (2014) 5322.
[44] J. Liang, G. Zhang, W. Sun, P. Dong, High efficiency flexible fiber-type dye-sensitized solar cells with multi-working electrodes, Nano Energy, 12 (2015) 501-509.
[45] S. Prasad, D. Devaraj, R. Boddula, S. Salla, M.S. AlSalhi, Fabrication, device performance, and MPPT for flexible dye-sensitized solar panel based on gel-polymer phthaloylchitosan based electrolyte and nanocluster CoS2 counter electrode, Materials Science for Energy Technologies, 2 (2019) 319-328.
[46] G. Yue, X. Liu, Y. Chen, J. Huo, H. Zheng, Improvement in the photoelectric conversion efficiency for the flexible fibrous dye-sensitized solar cells, Nanoscale research letters, 13 (2018) 188-188.
[47] Y. Xiao, J. Wu, G. Yue, J. Lin, M. Huang, L.-Q. Fan, Z. Lan, Preparation of a three-dimensional interpenetrating network of TiO2 nanowires for large-area flexible dye-sensitized solar cells, RSC Adv., 2 (2012) 10550-10555.
[48] J. An, W. Guo, T. Ma, Enhanced Photoconversion Efficiency of All-Flexible Dye-Sensitized Solar Cells Based on a Ti Substrate with TiO2 Nanoforest Underlayer, Small, 8 (2012) 3427-3431.
[49] K.C. Sun, I.A. Sahito, J.W. Noh, S.Y. Yeo, J.N. Im, S.C. Yi, Y.S. Kim, S.H. Jeong, Highly efficient and durable dye-sensitized solar cells based on a wet-laid PET membrane electrolyte, Journal of Materials Chemistry A, 4 (2016) 458-465.
[50] F. Bella, D. Pugliese, L. Zolin, C. Gerbaldi, Paper-based quasi-solid dye-sensitized solar cells, Electrochimica Acta, 237 (2017) 87-93.
[51] A. Lamberti, A. Virga, A. Angelini, A. Ricci, E. Descrovi, M. Cocuzza, F. Giorgis, Metal–elastomer nanostructures for tunable SERS and easy microfluidic integration, RSC Advances, 5 (2015) 4404-4410.
[52] S.H. Roelofs, A. van den Berg, M. Odijk, Microfluidic desalination techniques and their potential applications, Lab on a Chip, 15 (2015) 3428-3438.
[53] F. Bella, A. Lamberti, S. Bianco, T. Elena, C. Gerbaldi, C. Pirri, Floating Photovoltaics: Floating, Flexible Polymeric Dye-Sensitized Solar-Cell Architecture: The Way of Near-Future Photovoltaics (Adv. Mater. Technol. 2/2016), Advanced Materials Technologies, 1 (2016).
[54] M. Paulose, K. Shankar, O.K. Varghese, G.K. Mor, B. Hardin, C.A. Grimes, Backside illuminated dye-sensitized solar cells based on titania nanotube array electrodes, Nanotechnology, 17 (2006) 1446-1448.

[55] L.-C. Chen, C.-T. Hsieh, Y.-L. Lee, H. Teng, Electron Transport Dynamics in TiO2 Films Deposited on Ti Foils for Back-Illuminated Dye-Sensitized Solar Cells, ACS Applied Materials & Interfaces, 5 (2013) 11958-11964.
[56] D. Kuang, J. Brillet, P. Chen, M. Takata, S. Uchida, H. Miura, K. Sumioka, S.M. Zakeeruddin, M. Gratzel, Application of highly ordered TiO2 nanotube arrays in flexible dye-sensitized solar cells, Acs Nano, 2 (2008) 1113-1116.
[57] H. Wang, J. Fu, C. Wang, R. Zhang, Y. Li, Y. Yang, H. Li, Q. Sun, H. Li, Foldable high-strength electrode enabled by nanosheet subunits for advanced sodium-ion batteries, InfoMat, n/a (2021).
[58] D.-H. Kim, J.H. Kim, H.-K. Lee, J.-Y. Na, S.-K. Kim, J.H. Lee, S.-W. Kim, Y.-Z. Yoo, T.-Y. Seong, Flexible and transparent TiO2/Ag/ITO multilayer electrodes on PET substrates for organic photonic devices, Journal of Materials Research, 30 (2015) 1593-1598.
[59] B. Liu, D. Deng, J.Y. Lee, E.S. Aydil, Oriented single-crystalline TiO2 nanowires on titanium foil for lithium ion batteries, Journal of Materials Research, 25 (2010) 1588-1594.
[60] G. Boschloo, J. Lindstrom, E. Magnusson, A. Holmberg, A. Hagfeldt, Optimization of dye-sensitized solar cells prepared by compression method, Journal of Photochemistry and Photobiology a-Chemistry, 148 (2002) 11-15.
[61] T. Yoshida, T. Oekermann, K. Okabe, D. Schlettwein, K. Funabiki, H. Minoura, Cathodic Electrodeposition of ZnO/eosinY hybrid thin films from dye added zinc nitrate bath and their photoelectrochemical characterizations, Electrochemistry, 70 (2002) 470-487.
[62] X.J. Fan, D.P. Demaree, J.M.S. John, A. Tripathi, S.R.J. Oliver, Double-layer porous TiO2 electrodes for solid-state dye-sensitized solar cells, Appl. Phys. Lett., 92 (2008) 193108.
[63] L. Chu, Z. Qin, J. Yang, X.a. Li, Anatase TiO2 Nanoparticles with Exposed {001} Facets for Efficient Dye-Sensitized Solar Cells, Scientific Reports, 5 (2015) 12143.
[64] Ö. Birel, S. Nadeem, H. Duman, Porphyrin-Based Dye-Sensitized Solar Cells (DSSCs): a Review, Journal of Fluorescence, 27 (2017) 1075-1085.
[65] L. Sheng, G. Li, W. Zhang, K. Wang, Full-stainless steel mesh dye-sensitized solar cells based on core-shell ZnO/TiO2 nanorods, Optik, 184 (2019) 90-97.
[66] M.G. Brik, I.V. Kityk, Modeling of lattice constant and their relations with ionic radii and electronegativity of constituting ions of A2XY6 cubic crystals (A=K, Cs, Rb, Tl; X=tetravalent cation, Y=F, Cl, Br, I), Journal of Physics and Chemistry of Solids, 72 (2011) 1256-1260.